Synthesis, Docking, and Evaluation of Antimicrobial Activity of a New Series of Acyclo C-Nucleosides of 1, 2, 4-Triazolo[4, 3-*a*]quinoxaline Derivatives

Mohammed Salah Ayoup,[a] Hany Emary Ali Ahmed,[b,c]* Abdel Moneim El Massry,[a,d] Samir Senior,[a,d] Sherine Nabil Khattab,[a] Seham Yassen Hassan,[a] and Adel Amer[a,e]*

[a]Department of Chemistry, Faculty of Science, Alexandria University, P.O. Box 426 Ibrahimia, Alexandria, Egypt
[b]Pharmacognosy and Pharmaceutical Chemistry Department, Pharmacy College, Taibah University, Al-Madinha Al-Munawarah, Saudi Arabia
[c]Pharmaceutical Organic Chemistry Department, Faculty of Pharmacy, Al-Azhar University, Cairo, Egypt
[d]Department of Chemistry, College of Sciences and Arts, Rabigh Campus, King Abdulaziz University, Jeddah, Saudi Arabia
[e]Department of Chemistry, Faculty of Science, Taibah University, Al-Madinha Al-Munawarah, Saudi Arabia
*E-mail: adel.amer@alex-sci.edu.eg; heahmad@taibahu.edu.sa

Received August 19, 2014
DOI 10.1002/jhet.2396
Published online 00 Month 2015 in Wiley Online Library (wileyonlinelibrary.com).

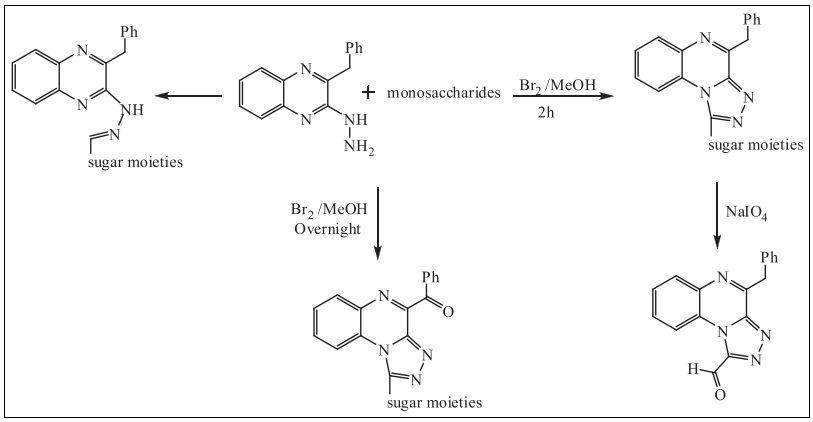

In this study, 18 new 3-benzylquinoxalinyl hydrazones bearing carbohydrate moiety and their corresponding triazoloquinoxalines were synthesized in order to investigate their possible antibacterial and antifungal activities. Some of these compounds such as **4b**, **4c**, **7b**, **7c,** and **7d** showed promising antibacterial and antifungal activities and were found to have more potent activity compared with that of standard drugs. From structure–activity relationship point of view, increasing the size of the substitutions at position 6 or 7 on the quinoxaline nucleus decreased the antimicrobial activity, while the presence of the hydroxyl groups at C2 (R) and C3 (S) of sugar moieties enhanced the activity. Further, molecular docking studies of the active compounds were performed on different targets belonging to different microorganisms and showed good scoring with further understanding of the various interactions with the active sites of interesting enzymes compared with the co-crystallized ligands.

J. Heterocyclic Chem., **00,** 00 (2015).

INTRODUCTION

In common with other nitrogen heterocycles, quinoxalines, as well as their fused-ring bio-isosteric analogues, show marked activity in many biological systems. A large number of compounds incorporating these ring systems were found to possess antibacterial activities. Thus, naturally occurring quinoxaline antibiotics are produced by several species of streptomycetes. They are characterized by a heterodetic cyclic octadepsipeptide to which two quinoxaline-2-carboxylic acid chromophores are attached, for example, Echinomycin [1]. Furthermore, several synthetic quinoxalines such as [1,2,4] triazolo[4,3-a]quinoxaline **I** [2–4] and quinoxalinone **II** derivatives [5–8] have shown activity against Gram-positive and Gram-negative microorganisms.

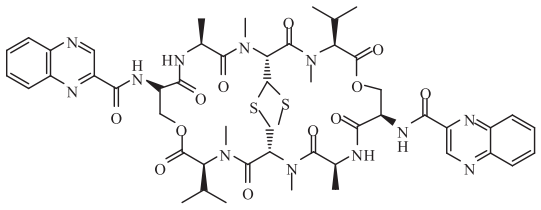

Echinomycin

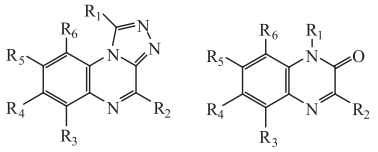

I **II**

Although many antibiotics are available to clinicians, many efforts have been invested in the search for novel agents with new mechanisms of action to address the need for new therapies to combat resistant organisms. Nucleosides are one class of compounds worthy of further investigation as antibacterial because some derivatives have shown moderate to good activity against specific bacterial strains [9–11].

In the course of our ongoing studies aimed at the synthesis heterocyclic compounds of potential pharmaceutical relevance, we were interested in synthesizing novel cyclo and acyclo C-nucleosides quinoxaline derivatives from 2-hydrazino-3-benzylquinoxaline **1** as the heterobase builder because of its involvement in several biological activities [12–15]. The antibacterial potency of these compounds prompted us to continue our investigation on quinoxalines in order to achieve additional data for a structure–activity relationship (SAR) study. In this context, we have prepared a new series of quinoxalin-2-yl sugar hydrazones bearing either benzyl or phenyl group in 3, or alternatively, chlorine atoms in 6 and 7 positions of quinoxaline nucleus. Furthermore, we studied their transformation to 1, 2, 4-triazolo-[4, 3-*a*]quinoxaline analogues in order to verify if this type of biological activity was maintained or not on the quinoxaline scaffold. The length of the carbohydrate moiety (namely, hexoses and pentoses) was also investigated. The procedures of preparation, identification, and screening the new series of compounds for their preliminary antimicrobial activity are described in this article.

RESULTS AND DISCUSSION

Chemistry. The sugar hydrazones **4–6** were obtained by the condensation of quinoxaline hydrazine derivatives **1–3** with different monosaccharides under the same reaction condition reported earlier [12]. Oxidative cyclization of compounds **4–6** with bromine in methanol gave corresponding fused triazoloquinoxalines **7–9** in good yield (Scheme 1). Analytically pure triazoloquinoxalines **7–9** were obtained by recrystallisation from appropriate solvents (see the Experimental section). Their structural proof was based on correct elemental analyses as well as on IR and NMR spectral data.

In our attempt to transform **1** to triazoloquinoxaline in one pot, D-mannose was selected as a prototype for a short and a long period oxidative-cyclization duration. Thus, when **1** was allowed to react with D-mannose in boiling acidified ethanolic medium for 1 h, cooled to room temperature then treated with methanolic bromine solution for 2 h, it afforded **7a**, which upon periodate oxidation afforded the quinoxaline carbaldehyde **10**. On the other hand, leaving the reaction mixture in methanolic bromine solution overnight gave after the work up (see the Experimental section) colorless crystals of **11** with melting points 227–228°C (Scheme 2). The ^{1}H-NMR of **11** showed no signal for the benzylic protons, while in ^{13}C-NMR spectrum, a signal at 190.91 ppm appeared for a carbonyl carbon atom. This type of benzylic carbon oxidation was reported to proceed through one-pot tandem halogenation-hydrolysis [16].

Scheme 2

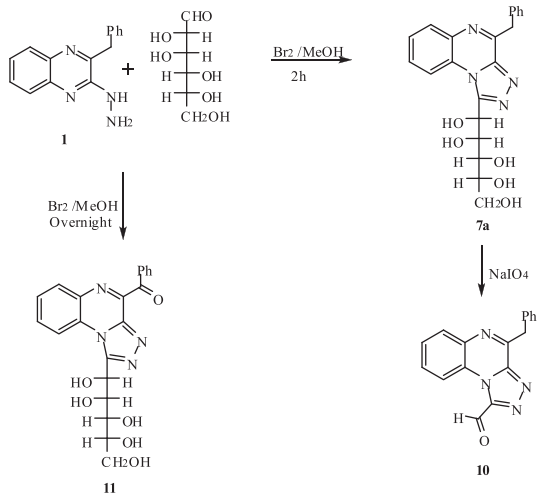

Scheme 1

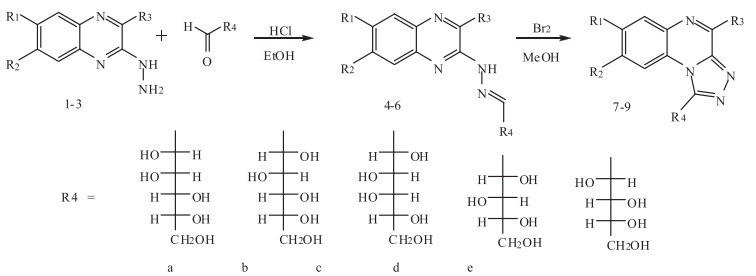

	R_1	R_2	R_3
1,4,7	H	H	$PhCH_2$
2,5,8	H	H	Ph
3,6,9	Cl	Cl	$PhCH_2$

In the present work, D-fructose hydrazone **12** was synthesized as ketose prototype. Its tautomeric forms were fully investigated by NMR and DFT quantum chemical calculations. The 500 MHz ^{1}H-NMR of compound showed the presence of only two isomeric forms in 1:3 ratio from the integrated D_2O exchangeable singlet peaks for N–H at 10.96 and 11.10 ppm. Its ^{13}C-NMR showed 10 signals (2×5) in the aliphatic region of the sugar part in addition to two signals at 171.32 and 169.54 ppm, which were assigned to C=N of open forms of syn and anti configurations.

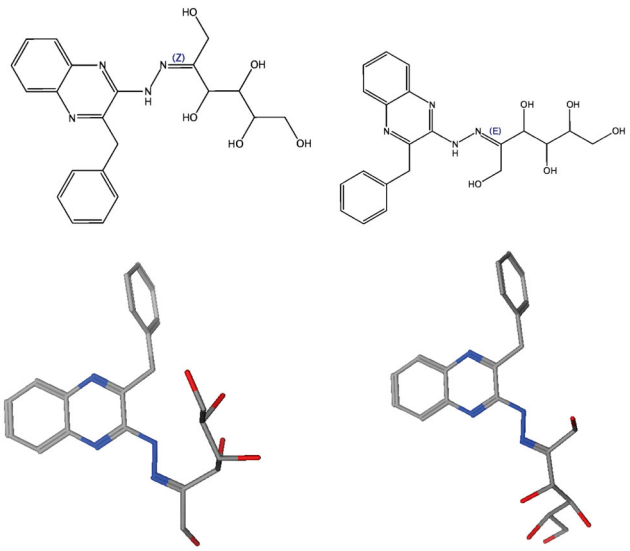

According to the total energy calculation in DMSO, as a solvent, the most stable two tautomers found are the open syn-isomer and the open anti-isomer. It is found that the open anti-isomer is more stable than the open syn-isomer by 2.512 kcal/mol.

Biological evaluation (antimicrobial activity inhibition). Final products were tested for their *in vitro* growth inhibitory activity against human pathogens. The utilized test organisms were *Escherichia coli* ATCC 8739, *Pseudomonas aeruginosa* ATCC 9027 as Gram-negative bacteria (Gm−ve), *Staphylococcus aureus* ATCC 6583P as an example of Gram-positive bacteria (Gm+ve), and *Candida albicans* ATCC 2091 as yeast-like fungi. Ampicillin, Ciprofloxacin, Clotrimazole, Dermatin, Erythromycin, and Imipenam were used as control drugs. The observed inhibition zone (IZ) antimicrobial data of the compounds and the reference drugs are given in Table 1. Lead compound **1** exhibited weak antibacterial and antifungal activities with IZ ranges between 17 and 25. Slight modification on substituents of quinoxaline moiety from benzyl-to-phenyl as **2** and hydrogen-to-chloro as **3** leads to slight improvement in their antibacterial (Gm−ve) and antifungal activities. The hydrazones **4a–d** showed significant increase in antibacterial and antifungal activities. This means the polar sugar fragments might be essential for the activity. Compound **4c** bearing D-galactose moiety has a prominent and potent antibacterial (Gm−ve) and antifungal activities. Its oxidative cyclization product **7c** showed similar activities. Compound **7b** bearing D-glucose moiety showed a potent and selective antifungal activity, while **7d** with D-xylose moiety possessed potent and selective antibacterial (Gm+ve) activity. As a result the SAR analysis of the synthesized compounds renders certain factors that affect their biological activities such as substituents at the 3, 5 and 6 positions and the length of sugar moiety.

Molecular modeling studies. ***Potential energy distribution of active compounds.*** Total molecular energy descriptors were calculated to structurally compare the active compounds. These energy descriptors accounted for different types of energy like torsion, electrostatic, and van der Waals (VDW) types. The comparison is reported in (Table 2) and full overview about their stability was given. Distribution of the energy of representative compounds showed low potential energy for some compounds like **4b**, **7b**, and **7d,** while in some degrees, the others are higher over 100 kcal/mol. These compounds with slight higher energy have some instability performance in the active site because they have higher extent of VDW energy and hence have low tolerability in the enzyme active site (Table 2).

Docking. Different biological targets found in bacteria and fungi are considered of medicinally interest. Because of the pharmacological profile as primary investigation of growth inhibition of microorganisms of test compounds and structural similarities for reference ligands, we decided to run molecular modeling studies using these three different biological targets as promising and pharmaceutical relevant targets for most of marketed drugs. We assumed here that compound derivatives might demonstrate their inhibition activity through interaction with three microbial targets belonging to Gm+ve and Gm−ve bacteria, and finally fungi. These target enzymes were chosen as major antimicrobial drug targets and essential for biological process in the microorganism cell life, and inhibition of such enzymes leads to overall cell death. We assumed here that compound derivatives might demonstrate their inhibition activity through interaction with three microbial targets belonging to Gm+ve and Gm−ve bacteria, and finally fungi. These target enzymes were chosen as major antimicrobial drug targets and essential for biological process in the microorganism cell life and inhibition of such enzymes leads to overall cell death. Through the docking work, the representative compounds showed different docking scores ranging between −12.00 as low binding character to −17.66 kcal/mol as strong binding effect (Table 3). The difference in the scores reflects the ability of the compounds to tolerate the active site of the enzyme. However, they exhibit

Table 1

Antimicrobial activity (inhibition zone profiles) of the synthesized compounds.

	Inhibition zone			
	Antibacterial activity			Antifungal activity
	G(+ve)	G(−ve)		
Compound	*Staphylococcus aureus*	*Pseudomonas aeruginosa*	*Escherichia coli*	*Candida albicans*
1	25	17	20	20
2	23	23	19	25
3	23	18	22	24
4a	8	7	25	27
4b	14	15	32	31
4c	19	17	35	34
4d	29	10	12	29
4e	—	20	22	—
12	28	8	9	28
7a	23	21	—	—
7b	21	19	39	39
7c	13	11	31	30
7d	36	18	20	37
7e	—	22	24	—
5a	23	20	21	22
5b	22	25	21	25
8a	24	20	20	24
8b	25	18	19	25
8c	23	21	19	22
6a	25	17	17	19
6b	25	18	20	24
6c	25	19	21	20
9a	23	17	18	19
9b	20	18	18	18
9c	23	18	18	19
CPF	30	38	25	—
CZL	—	—	—	29

Gm(+ve), Gram-positive bacteria; G(−ve), Gram-negative bacteria; CPF. ciprofloxacin drug; CZL, clotrimazole.

Table 2

Potential energy for representative compounds.

Compound	Total energy	Torsion energy	VDW	Electrostatic energy
4b	102	9.06	60.50	0.00
4c	104	10.8	62.80	0.00
4d	123	5.66	54.09	34.76
7b	93	12.96	61.29	−5.74
7c	106	13.27	69.07	−1.00
7d	91	10.2	50.3	6.8

VDW, van der Waals force.

mostly similar binding mode to the reference ligands that makes these compounds possibly having the same mechanism of action. The next sections explained their binding mechanisms compared with the co-crystallized ligands.

Docking work against Gm−ve bacteria (E. coli). The main goal of this docking work was to explore how candidate molecules work and investigate their binding modes at the active site. In the target protein, docking of the reference ligand showed different types of interactions, H-bonding with amino acid residues lle192, Ala196, Asp64, and Lys163. In addition, the tight

Table 3

Docking scores for representative compounds.

	Docking score			Inhibition zone		
Compound	AD4	1KMM	1IYL	*Staphylococcus aureus*	*Escherichia coli*	*Candida albicans*
4b	−15.25	−17.66	−17.13	14	32	31
4c	−13.90	−16.60	−16.32	19	35	34
4d	−14.70	−13.50	−15.04	29	12	29
7b	−12.80	−14.80	−14.74	21	39	39
7c	−13.40	−15.70	−14.9	13	31	30
7d	−16.90	−13.30	—	36	20	—

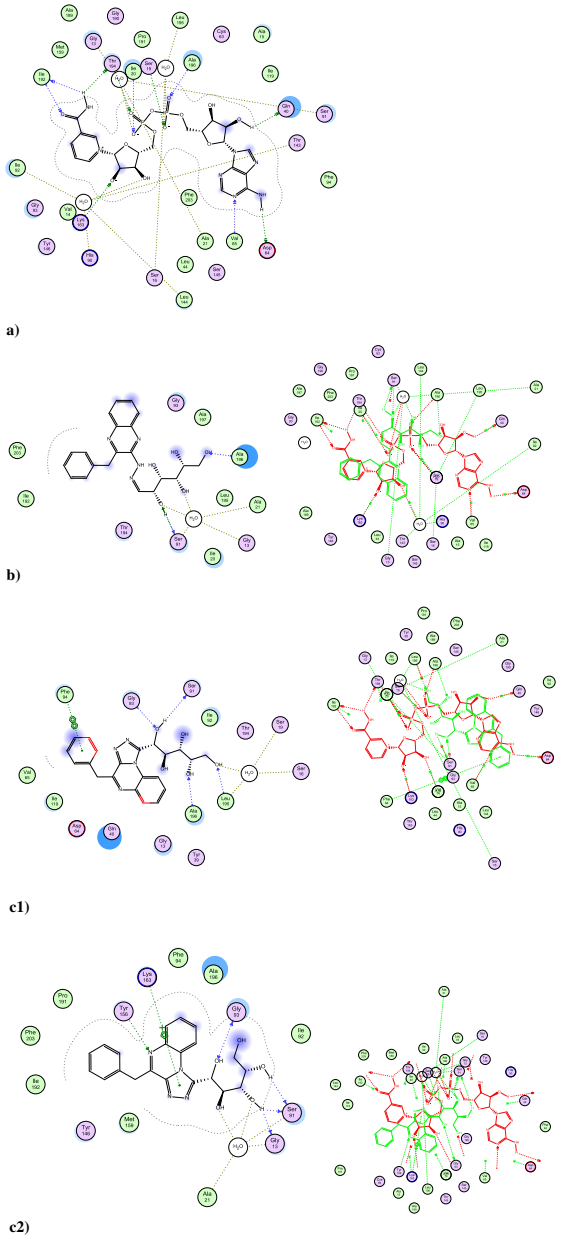

Figure 1. 2D depiction of the docked conformation of the most active compound: (a) reference ligand bound to the target protein (enoyl-acyl carrier protein reductase (FabI) (PDB code 1C14)); (b) compound **4c** in the active site of the enzyme; (c) compound **7b–c** in the active site of the enzyme. Both ligands reference and active compounds are aligned in the binding pocket and compared in each figure. [Color figure can be viewed in the online issue, which is available at wileyonlinelibrary.com.]

positioning of pyridine ring in a hydrophobic pocket form of lle92, lle192, Phe203, and Val14 gives good filing of ligand in the active site. Compounds **4c**, **7b,** and **7c** were docked and compared. The phenylquinoxaline moiety adopted an appropriate orientation to form a π–π stacking (hydrophobic aromatic) with the lle92, lle192, and Phe203 residues pocket. In addition, hydrogen-bonding interactions of sugar side chain OHs of target compounds **4c**, **7b,** and **7c** with Ser91, Ala196, and Gly93 amino acid residues that similar to reference ligand were detected. Finally, they could have a strong resemblance to the reference ligand and thus might have the same mode of action as antibacterial agents (Fig. 1a–c).

Docking work against Gm+ve bacteria (S. aureus). In this case, docking studies were also performed for compound **7d** utilizing dihydropteroate synthetase as promising target of *S. aureus* bacteria. The compound **7d** was reported most active against *S. aureus*. Docking of **7d** showed strong hydrogen-bonding interaction with Arg52 and Gln105 residues similar to the reference one. In

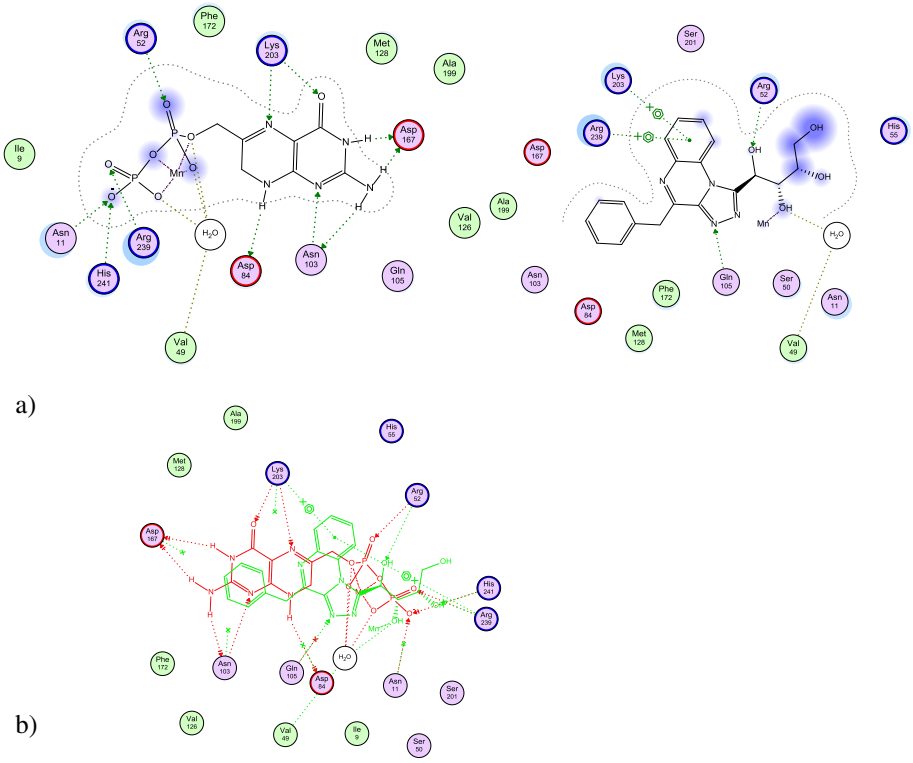

Figure 2. 2D depiction of the docked conformation of the most active compound: (a) reference ligand bound to the target protein (dihydropteroate synthetase (PDB code 1 AD4)); (b) compound **7d** in the aligned at the binding pocket. [Color figure can be viewed in the online issue, which is available at wileyonlinelibrary.com.]

addition, it exhibited indirect H_2O-dependent metal interaction through the backbone Val49. Also, the appearance of hydrophobic stable binding of quinoxaline moiety with the two amino acids Lys203 and Arg239 was detected. Thus, compound **4d** could cause its activity because of the similar adopting of binding mode of co-crystallized ligand (Fig. 2a–b).

Docking work against fungi (C. albicans). The binding mode of the most compounds **4b**, **4c**, **7b**, and **7c** against *C. albicans* with the active site of *N*-myristoyl transferase (CaNmt) is shown in Figure 3. The benzyl quinoxaline ring was located at the center of the active site, surrounded by some hydrophobic residues, such as Phe117, Phe339, Phe240, Val108, and Tyr335. Because the OH groups of aliphatic sugar side chain was important for the activity because of the ability to form stable hydrogen-bonding interaction with Tyr107 and Asn175 residues. However, it has been confirmed that Leu451 is an important functional residue in the catalytic cycle of CaNmt, and the docking results revealed that the sugar side-chain OHs made a strong hydrogen bond with C-terminal carboxylate of Leu451, which was consistent with the binding mode of reference ligand. An extra aromatic hydrophobic interaction was exhibited through Tyr225 residue with the benzyl quinoxaline fragment that strengthens the ligand interaction (Fig. 3a–d).

CONCLUSIONS

In summary, we have synthesized a series of acyclo C-nucleosides of 1, 2, 4-triazolo[4,3-a]quinoxaline derivatives and evaluated for their *in vitro* antimicrobial activities that were successfully achieved. Five compounds **4c**, **4d**, **7b**, **7c,** and **7d** showed excellent antibacterial activities against all the tested strains with IZ value comparable with those of ciprofloxacin and clotrimazole. Specially, compound **7d** displayed high Gm+ve antimicrobial and antifungal inhibitory activity. From SAR point of view, increasing the size of the substitutions at position 6 or 7 on the quinoxaline nucleus decreased the antimicrobial activity, while the presence of the hydroxyl groups at C2 (R) and C3 (S) of sugar moieties enhanced the activity. Computational molecular analyses were carried out and helped in exploring SARs of the candidate molecules with comparative docking and potential energy scores and proved that derivatives have ability to inhibit a panel of microorganisms. Detailed molecular docking studies further supported the inhibitory activity of target compounds and further help in understanding the various interactions between the ligands and enzyme active sites. As a result, three different activity profiles involving potent bivotal anti-Gm+ve antifungal drugs, anti-Gm−ve antifungal compounds, and potent antifungal drugs have been introduced:

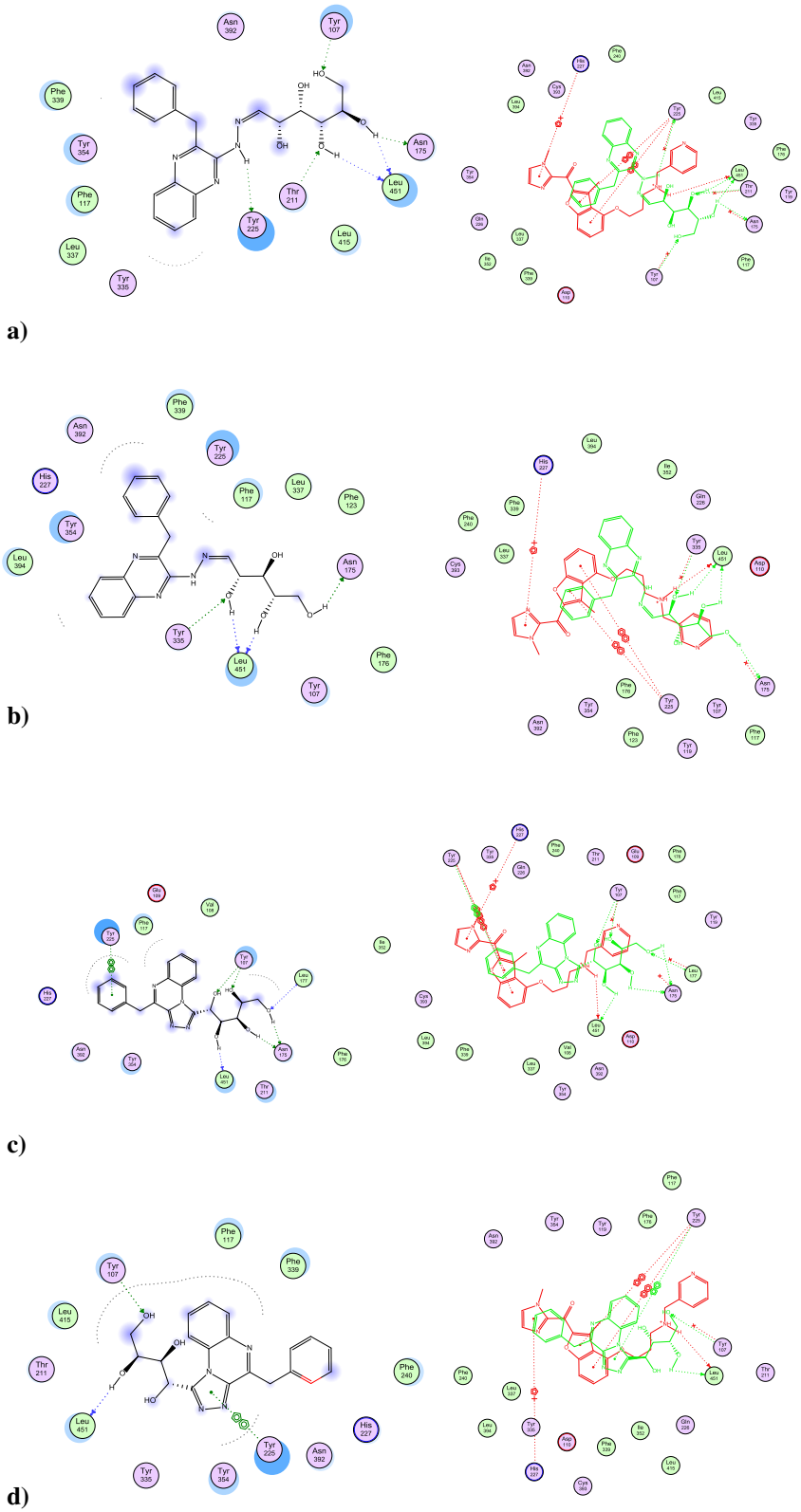

Figure 3. 2D depiction of the docked conformation of the most active compounds: (a) compound **4b** in the aligned at the binding pocket to the target protein (*N*-myristoyl transferase (PDB code 1IYL); (b) compound **4c** in the aligned at the binding pocket; (c) compound **7b** in the aligned at the binding pocket; and (d) compound **7c** in the aligned at the binding pocket. Each compound is depicted in aligned form with the reference one. [Color figure can be viewed in the online issue, which is available at wileyonlinelibrary.com.]

compounds **7a**, **7b,** and **7d**. They may be considered as a promising leads for future design of potent and selective antimicrobial agents.

EXPERIMENTAL

Chemistry. Melting points were obtained in open capillary tubes by using a MEL-Temp II melting point apparatus (Cole Parmer, Dubuque, Iowa, USA) and are uncorrected. TLC was performed using aluminum-backed Merck Silica Gel 60 F254 plates (Sigma-Aldrich, Seelze, Germany), with UV 254 nm, 20 × 20 cm, 2000 µm using suitable solvent systems with spots being visualized by a Spectroline UV Lamp (254 or 366 nm; Sigma-Aldrich, Seelze, Germany) or staining by I_2 vapor. IR spectra were recorded on a Perkin-Elmer 1600 series Fourier transform instrument (Perkin-Elmer, Waltham, MA, USA) as KBr pellets, the absorption bands (ν_{max}) cm^{-1}. ^{1}H-NMR and ^{13}C-NMR were recorded on JOEL 500 MHz spectrometers (JEOL, Tokyo, Japan) at ambient temperature and reported for the major isomer (when applicable). Mass spectra were recorded on a JOEL JMS AX-500 spectrometer (JEOL) by using EI at 70 eV. Compounds **1–3** were synthesized following the procedures described earlier [15,17]. Compounds **4a–c** and **7a–c** were prepared as previously reported [12].

General procedures for the preparation of D-sugar (2-hydrazinoquinoxaline derivatives) hydrazones. To a solution of the hydrazine **1–3** (2.5 mmol) ethanol (25 mL), the corresponding sugar (2.5 mmol) was added and one drop of HCl (33%). The reaction mixture was heated under reflux for 1 h then left to cool to room temperature. The solid that separated out was filtered off, washed with ethanol, and dried.

D-Xylose (3-benzylquinoxalin-2-yl) hydrazone (4d). This compound was obtained as pale red crystals; (0.6 g, 63%); with mp 179–180°C; R_f 0. 55 (7:3 ethylacetate to *n*-hexane). IR (KBr); ν 3376 (NH, OH) and 1660 cm^{-1} (C=N); ^{1}H-NMR (DMSO-d_6, 500 MHz): δ 3.52–3.62 (m, 3H, H-4`, H-5`$_a$, H-5`$_b$), 4.06 (s, 2H, $PhCH_2$), 4.35–4.39 (m, 1H, H-2`), 4.46–4.61 (m, 4H, H-3`, OH-3`, OH-4`, OH-5`, exchangeable with D_2O), 5.13 (d, $J_{OH2`,2`}$ 5.3 Hz, OH-2`, exchangeable with $D_2O$), 7.15 (m, 1H, Ph-H,), 7.22–7.34 (m, 6 H, quin-$H_7$, quin-$H_8$, Ph-H), 7.48 (d, 1 H, $J_{6,7}$ 7.6 Hz, quin-$H_6$), 7.68 (m, 1 H, quin-$H_9$), 7.88 (d, 1H, $J_{1`,2`}$ 4.5 Hz, H-1`), 10.97 (s, 1H, N–H, exchangeable with D_2O), ^{13}C-NMR (DMSO-d_6, 125.7 MHz): δ 40.0 ($PhCH_2$,), 63.02, 72.10, 72.37, 72.58, 122.55, 126.81, 128.55, 128.65, 128.75, 129.51, 129.73, 132.29, 132.65, 137.83, 137.59, 137.91, 138.30, 138.66, 140.17, 145.88, 147.78, 151.33(aromatic carbons for the major isomer), 160.87 (C-1`). *Anal.* Calcd for $C_{20}H_{22}N_4O_4$: C, 62.82; H, 5.80; N, 14.65, Found: C, 62.96; H, 6.01; N, 14.82.

D-Arabinose (3-benzylquinoxalin-2-yl) hydrazone (4e). This compound was obtained as deep yellow crystals that precipitated out that was collected by filtration to yield (0.66 g; 69.45%); with mp 175–176°C; R_f 0. 5 (7:3 ethylacetate to *n*-hexane). IR (KBr); ν 3283 (NH, OH) and 1632 cm^{-1} (C=N). *Anal.* Calcd for $C_{20}H_{22}N_4O_4$: C, 62.82; H, 5.80; N, 14.65, Found: C, 63.02; H, 5.91; N, 14.35.

D-Mannose (3-phenylquinoxalin-2-yl) hydrazones (5a). This compound was obtained as deep yellow crystals, (0.90 g; 89%); mp 242–243°C; R_f 0.6 (7:3 ethylacetate: *n*-hexane). ^{1}H-NMR (DMSO-d_6, 500 MHz): δ 3.65–3.86 (m, 4H, H-4`, H-5`, H-6`$_a$, H-6`$_b$), 4.39–4.43 (m, 1H,O H-6`, exchangeable with $D_2O$), 4.52–4.57 (m, 5H, H-3`, OH-2`, OH-3`, OH-4`, OH-5`, exchangeable with D_2O), 5.50–5.53 (m, 1H, H-2`), 6.46 (d, $J_{OH2`,2`}$ 5.3 Hz, 1H, OH-1`, exchangeable with D_2O), 7.61 (bs, 3H, Ph-H,), 7.70–7.80 (m, 2H, Ph-H, H-1`), 8.14–8.17 (m, 1 H, quin-H_6), 8.73 (bs, 2H, quin-H_7, quin-H_8), 8.81–8.79 (m, 1H, quin-H_9), 10.20 (s, 1H, N–H, exchangeable with D_2O). *Anal.* Calcd for $C_{20}H_{22}N_4O_5$: C, 60.29; H, 5.57; N, 14.06 Found: C, 60.44; H, 5.32; N, 13.82.

D-Glucose (3-phenylquinoxalin-2-yl) hydrazones (5b). This compound was obtained as deep red crystals, (0.94 g; 92%); mp 149–150°C; R_f 0.7 (7:3 ethylacetate: *n*-hexane). ^{1}H-NMR (DMSO-d_6, 500 MHz): δ 2.99–3.66 (m, 3H, H-5`, H-6`$_a$, H-6`$_b$), 4.61–4.63 (dis. d, 1H, H-4`), 4.86–4.88 (m, 5H, H-3`, OH-3`, OH-4`, OH-5`, OH-6`, exchangeable with $D_2O$), 5.48–5.50 (d, *J* 5.3 Hz, 1H, H-2`), 5.64 (s, 1H, OH-2`, exchangeable with $D_2O$), 7.14–7.17 (m, 1H, Ph-H,), 7.39–7.52 (m, 3H, Ph-H), 7.59–7.60 (m, 2H, H-1`, quin-H_6), 7.67–7.79 (m, 2H, quin-H_7, quin-H_8), 8.70–8.77 (m, 1H, quin-H_9), 10.17 (s, 1H, N–H, exchangeable with D_2O). *Anal.* Calcd for $C_{20}H_{22}N_4O_5$: C, 60.29; H, 5.57; N, 14.06. Found: C, 59.78; H, 5.29; N, 14.12.

D-Mannose (3-benzyl-6,7-dichloroquinoxalin-2-yl) hydrazones (6a). This compound was obtained as deep yellow crystals, (0.80 g; 66.6%); mp 180–181°C; R_f 0.4 (7:3 ethylacetate: *n*-hexane): ^{1}H-NMR (DMSO-d_6, 500 MHz): δ 3.91–5.68 (m, CH and OH of sugar moiety), 4.05 (bs, 2H, $PhCH_2$), 7.29 (dist. t, 1H, Ph-H), 7.53 (m, 4H, Ph-H), 7.80 (s, 1H, quin-H_6), 7.92 (d, 1H, H-1`), 8.06 (s, 1H, quin-H_9), 9.20 (s, 1H, N–H, exchangeable with D_2O). *Anal.* Calcd for $C_{21}H_{22}C_{l2}N_4O_5$: C, 52.40; H, 4.61; N, 11.64 Found: C, 53.18; H, 5.69; N, 11.42.

D-Glucose (3-benzyl-6,7-dichloroquinoxalin-2-yl) hydrazones (6b). This compound was obtained as deep reddish yellow crystals, (1.10 g, 91%); mp 225–226°C; R_f 0.77 (7:3 ethylacetate: *n*-hexane): ^{1}H-NMR (DMSO-d_6, 500 MHz): 7.17 (dist. t, 1H, Ph-H,), 7.23–7.26 (m, 5H, Ph-H, H-1`), 7.39 (s, 1H, quin-H_6), 7.93 (s, 1H, quin-H_9), 9.24 (s, 1H, N–H, exchangeable with D_2O). *Anal.* Calcd for $C_{21}H_{22}C_{l2}N_4O_5$: C, 52.40; H, 4.61; N, 11.64 Found: C, 51.88; H, 5.18; N, 12.02.

D-Galactose (3-benzyl-6,7-dichloroquinoxalin-2-yl) hydrazones (6c). This compound was obtained as pale orange crystals, (1.0 g; 83%); mp 145–146°C; R_f 0.54 (7:3 ethylacetate: *n*-hexane): ^{1}H-NMR (DMSO-d_6, 500 MHz): δ 3.46–3.77 (m, 5H, H-4`, H-5`, H-6`$_a$, H-6`$_b$, OH-6`, exchangeable with $D_2O$), 4.07 (bs, 2H, $PhCH_2$), 4.26–4.28 (m, 1H, H-3`), 4.17–4.48 (m, 3H, OH-3`, OH-4`, OH-5`, exchangeable with $D_2O$), 4.87 (dis. d, 1H, H-2`), 6.10 (bs, OH-2`, exchangeable with $D_2O$), 7.17 (dist. t, 1H, *J* 7.6 Hz, *J* 6.9 Hz, Ph-H,), 7.23–7.28 (m, 4H, Ph-H), 7.33 (m, 1H, H-1`), 7.40 (s, 1H, quin-H_6) 7.86 (s, 1H, quin-H_9), 9.24 (s, 1H, N–H, exchangeable with D_2O). *Anal.* Calcd for $C_{21}H_{22}C_{l2}N_4O_5$: C, 52.40; H, 4.61; N, 11.64 Found: C, 53.11; H, 4.19; N, 11.92.

General procedure for the preparation of 1-(alditol-1-yl)-4-substituted-[1,2,4]triazolo[4,3-*a*]quinoxaline derivatives. To a solution of **1–3** (2.50 mmol) in methanol (25 mL), the corresponding sugar (2.50 mmol) and one drop of HCl (33%) were added. The reaction mixture was heated under reflux on boiling water bath for 1 h, left to cool at room temperature, and then a solution of bromine (0.13 mL, 2.50 mmol) in methanol (5.0 mL) was added drop wise with stirring, for 2 h. A mixture of ethanol (3 mL) and pyridine (0.5 mL) was added, volatile components were evaporated in vacuum at 60°C. The residue was treated with ethanol (95%, 10 mL), then left to cool at room temperature. The crude product that precipitated out was collected by filtration, washed by ethanol.

1-(D-Xylo-tetritol-1-yl)-4-benzyl[1,2,4]triazolo[4,3-a] quinoxaline (7d). The crude product was crystallized from methyl alcohol to give colorless crystals, (0.4 g; 42.1%); mp 209–210°C; R_f 0.66 (6:1 chloroform: methanol). IR (KBr); ν 3282 (OH), 1626 cm^{-1} (C=N); ^{1}H-NMR (DMSO-d_6, 500 MHz): δ 3.41 (dd, 1H, *J* 10.7 Hz, *J* 6.1 Hz,, H-4`$_a$), δ 3.49 (dd, 1H, *J* 10.7 Hz, *J* 5.35 Hz,, H-4`$_b$), 3.52–3.53 (m, 1H, H-3`), 4.30–4.34 (m, 1H, H-2`), 4.45–4.47 (m, 2H, OH-3`, OH-4`, exchangeable with D_2O), 4.54 (s, 2H, $PhCH_2$), 4.92 (d, 1H, $J_{OH\text{-}2`,2`}$ 6.1 Hz, OH-2`, exchangeable with $D_2O$), 5.43 (t, 1H, *J* 6.9 Hz, *J* 7.6 Hz, H-1`), 6.13 (d, 1H, $J_{OH\text{-}1`,1`}$ 6.85 Hz, OH-1`, exchangeable with D_2O), 7.1 (t, 1H, *J* 7.6 Hz, Ph-H), 7.24 (t, 2H, *J* 7.6 Hz, Ph-H), 7.43 (d, 2H, *J* 7.6 Hz, Ph-H), 7.64–7.73 (m, 2H, quin-H_7, quin-H_8), 8.0 (dist. t, 1H, *J* 7.6 Hz, *J* 1.5 Hz, quin-H_6), 8.63 (d, 1H, $J_{9,8}$ 8.4 Hz, quin-H_9). *Anal*. Calcd for $C_{20}H_{20}N_4O_4$: C, 63.15; H, 5.30; N, 14.73. Found: C, 63.17; H, 5.60; N, 14.35.

1-(D-Arabino-tetritol-1-yl)-4-benzyl[1,2,4]triazolo[4,3-a] quinoxaline (7e). The crude product was crystallized from ethanol 95% to give colorless crystals, (0.55 g; 57.6%); mp 205–206°C, R_f 0.67 (6:1 chloroform to methanol). IR (KBr); ν 3313 (OH), 1628 cm^{-1} (C=N); ^{1}H-NMR (DMSO-d_6, 500 MHz): δ 3.39 (dd, 1H, *J* 10.7 Hz, *J* 6.1 Hz, H-4`$_a$), δ 3.46 (dd, 1H, *J* 10.7 Hz, *J* 5.35 Hz,, H-4`$_b$), 3.52 (dist. t, *J* 6.9, *J* 5.35, 1H, H-3`), 4.31–4.35 (m, 1H, H-2`), 4.41–4.44 (m, 2H, OH-3`, OH-4`, exchangeable with D_2O), 4.55 (s, 2H, $PhCH_2$), 4.90 (d, 1H, $J_{OH\text{-}2`,2`}$ 6.1 Hz, OH-2`, exchangeable with $D_2O$), 5.41 (d, 1H, *J* 6.1 Hz, H-1`), 6.10 (s, 1H, OH-1`, exchangeable with D_2O), 7.18 (t, 1H, *J* 7.6 Hz, Ph-H), 7.26 (t, 2H, *J* 7.6 Hz, Ph-H), 7.44 (d, 2H, *J* 7.6 Hz, Ph-H), 7.66 (t, 1H, $J_{7,8}=J_{7,6}$ 6.9 Hz, quin-H_7), 7.73 (t, 1H, $J_{8,7}=J_{8,9}$ 6.9 Hz, quin-H_8), 8.03 (d, 1H, *J* 7.6 Hz, quin-H_6), 8.65 (d, 1H, $J_{9,8}$ 8.4 Hz, quin-H_9). *Anal*. Calcd for $C_{20}H_{20}N_4O_4$: C, 63.15; H, 5.30; N, 14.73. Found: C, 63.56; H, 4.59; N, 14.79.

1-(D-Manno-pentitol-1-yl)-4-phenyl[1,2,4]triazolo[4,3-a] quinoxaline (8a). The crude product was recrystallized from ethanol 95% to give colorless crystals, (0.61 g; 61%); mp 245–246°C; ^{1}H-NMR (DMSO-d_6, 500 MHz): δ 3.43–3.51 (m, 2H, H-5`$_a$, H-5`$_b$), 3.57 (m, 1H, H-4`), 3.83 (t, 1H, *J* 8.4 Hz, H-4`), 4.39–4.41 (m, 2H, OH-4`, OH-5`, exchangeable with D_2O), 4.46–4.51 (m, 2H, OH-3`, OH-2`, exchangeable with D_2O), 4.55 (dist. t, 1H, *J* 7.6 Hz, *J* 9.1 Hz, H-2`), 5.52 (dd, 1H, *J* 6.1 Hz, *J* 9.9 Hz, H-1`), 6.44 (bd, 1H, OH-1`, exchangeable with D_2O), 7.61 (t, 3H, *J* 3.0 Hz, Ph-H), 7.70–7.75 (m, 2H, Ph-H), 8.16 (dist. t, 1H, *J* 7.6 Hz, *J* 1.5 Hz, quin-H_6), 8.72–8.74 (m, 2H, quin-H_7, quin-H_8), 8.80 (d, 1H, $J_{9,8}$ 8.4 Hz, quin-H_9). *Anal*. Calcd for $C_{20}H_{20}N_4O_5$: C, 60.60; H, 5.09; N, 14.13; Found: C, 59.94; H, 5.52; N, 14.31.

1-(D-Gluco-pentitol-1-yl)-4-phenyl[1,2,4]triazolo[4,3-a] quinoxaline (8b). The crude product was recrystallized from ethyl alcohol to give colorless crystals, (0.71 g, 71%); mp 165–166°C; ^{1}H-NMR (DMSO-d_6, 500 MHz): δ 3.25–3.31 (m, 2H, H-5`$_a$, H-5`$_b$), 3.48–3.54 (m, 2H, H-3`, H-4`), 4.25 (t, 1H, *J* 5.3 Hz, OH-5`, exchangeable with $D_2O$), 4.33 (d, 1H, $J_{OH\text{-}4`,H4`}$ 5.3 Hz, OH-4`, exchangeable with D_2O) 4.41 (d, 1H, $J_{OH\text{-}3`,H3`}$ 7.6 Hz, OH-3`, exchangeable with $D_2O$), 4.92 (d, 1H, $J_{OH\text{-}2`,2`}$ 6.1 Hz, OH-2`, exchangeable with D_2O), 5.49 (d, 1H, *J* 7.6 Hz, H-1`), 6.18 (s, 1H, OH-1`, exchangeable with D_2O), 7.61 (t, 3H, *J* 3.05 Hz, Ph-H), 7.76 (m, 2H, Ph-H), 8.17 (d, 1H, $J_{6,7}$ 7.6 Hz, quin-H_6), 8.74 (m, 3 H, quin-H_7, quin-H_8, quin-H_9). *Anal*. Calcd for $C_{20}H_{20}N_4O_5$: C, 60.60; H, 5.09; N, 14.13; Found: C, 60.12; H, 5.12; N, 14.23.

1-(D-Galacto-pentitol-1-yl)-4-phenyl[1,2,4]triazolo[4,3-a] quinoxaline (8c). The crude product was recrystallized from ethyl alcohol to give white crystals, (0.85 g, 85%); mp 230–231°C; ^{1}H-NMR (DMSO-d_6, 500 MHz): δ 3.38–3.45 (m, 2H, H-5`$_a$, H-5`$_b$), 3.71 (t, 1H, *J* 8.4 Hz, H-3`), 3.80 (m, 1H, H-4`), 4.22–4.26 (m, 2H, H-2`, OH-3`, exchangeable with D_2O), 4.39 (d, 1H, $J_{OH\text{-}4`,H4`}$ 7.6 Hz, OH-4`, exchangeable with $D_2O$) 4.49 (dist. t, 1H, $J_{OH5`,\ 5`a}$ 5.35 Hz, $J_{OH5`,\ 5`b}$ 6.1 Hz, OH-5`, exchangeable with D_2O), 4.91 (d, 1 H, $J_{OH\text{-}2`,2`}$ 5.35 Hz, OH-2`, exchangeable with $D_2O$), 5.67 (d, 1H, *J* 8.4 Hz, H-1`), 5.97 (d, 1H, $J_{OH\text{-}1`,1`}$ 7.6 Hz, OH-1`, exchangeable with D_2O), 7.17 (dist. t, 1H, *J* 7.6 Hz, *J* 6.9 Hz, Ph-H), 7.61 (bs, 3H, Ph-H), 7.71 (t, 1H, *J* 7.6 Hz, Ph-H), 7.77 (t, 1H, *J* 7.6 Hz, Ph-H), 8.13 (d, 1H, $J_{6,7}$ 7.6 Hz, quin-H_6), 8.72 (bs, 2H, quin-H_7, quin-H_8), 8.82 (d, 1H, $J_{9,8}$ 8.4 Hz, quin-H_9), *Anal*. Calcd for $C_{20}H_{20}N_4O_5$: C, 60.60; H, 5.09; N, 14.13; Found: C, 59.88; H, 5.61; N, 14.21.

1-(D-Manno-pentitol-1-yl)-4-benzyl-7,8-dichloro[1,2,4] triazolo[4,3-a]-quinoxaline (9a). The crude product was recrystallized from ethanol 95% to give colorless crystals, (0.88 g; 74%); mp 201–202°C: ^{1}H-NMR (DMSO-d_6, 500 MHz): δ 3.30–3.36 (m, 2H, H-5`$_a$, H-5`$_b$ H-4`, H-3`), 3.68–3.74 (m, 2H, H-4`, H-3`), 4.04 (dist. t, 1H, $J_{OH5`,\ 5`a}$ 8.6 Hz, $J_{OH5`,\ 5`b}$ 6.1 Hz, OH-5`, exchangeable with $D_2O$), 4.19 (d, 1H, $J_{OH4`,H4`}$, 6.8 Hz, OH-4` `, exchangeable with $D_2O$), 4.37 (d, 1H, $J_{OH3`,\ H3`}$, 7.6 Hz, OH-3`, exchangeable with D_2O), 4.52–4.60 (m, 3H, H-2`, $PhCH_2$), 4.94 (d, 1H, $J_{2`,\ OH2`}$ 7.1 Hz, OH-2`, exchangeable with D_2O), 5.63 (dist. d, 1H, H-1`), 6.23 (d, 1H, $J_{1`,\ OH1`}$ 7.6 Hz, OH-1`, exchangeable with D_2O), 7.17 (dist. t, 1H, *J* 6.9 Hz, *J* 7.6 Hz, Ph-H) 7.25 (t, 2H, *J* 7.6 Hz, Ph-H), 7.41 (d, 2H, *J* 6.8 Hz, Ph-H), 8.22 (s, 1H, quin-H_6), 9.31 (s, 1H, quin-H_9). *Anal*. Calcd for $C_{21}H_{20}Cl_2N_4O_5$, C, 52.62; H, 4.21; N, 11.69. Found: C, 52.93; H, 3.86; N, 11.74.

1-(D-Gluco-pentitol-1-yl)- 4-benzyl-7,8- dichloro[1,2,4] triazolo [4,3-a]-quinoxaline (9b). The crude product was recrystallized from ethyl alcohol to give colorless crystals, (0.70 g, 59%); mp 220–221°C; ^{1}H-NMR (DMSO-d_6, 500 MHz): δ 3.28–3.34 (m, 2H, H-5`$_a$, H-5`$_b$), 3.49–3.53 (m, 2H, H-4`, H-3`), 4.31 (dist. t, 1H, $J_{OH5`,\ 5`a}$ 5.35 Hz, $J_{OH5`,\ 5`b}$ 4.5 Hz, OH-5`, exchangeable with $D_2O$), 4.42–4.46 (m, 3H, H-2`, $PhCH_2$), 4.53–4.54 (bd, 2H, OH-3`, OH-4`), 4.93 (d, 1H, $J_{2`,\ OH2`}$ 6.10 Hz, OH-2`, exchangeable with $D_2O$), 5.37 (dist. t, 1H, $J_{1`,\ OH1`}$ 6.1 Hz, $J_{1`,\ 2`}$ 7.6 Hz, H-1`), 6.36 (d, 1H, $J_{1`,\ OH1`}$ 5.3 Hz, OH-1`, exchangeable with D_2O), 7.18 (dist. t, 1H, *J* 6.8 Hz, *J* 7.6 Hz, Ph-H) 7.26 (t, 2H, *J* 7.6 Hz, Ph-H), 7.42 (d, 2H, *J* 7.6 Hz, Ph-H), 8.29 (s, 1H, quin-H_6), 8.92 (s, 1H, quin-H_9). *Anal*. Calcd for $C_{21}H_{20}Cl_2N_4O_5$, C, 52.62; H, 4.21; N, 11.69. Found: C, 52.01; H, 4.36; N, 11.77.

1-(D-Galacto-pentitol-1-yl)-4-benzyl-7,8-dichloro[1,2,4] triazolo[4,3-a]-quinoxaline (9c). The crude product was recrystallized from methyl alcohol to give bright gray crystals, (0.90 g, 75%); mp 245–246°C; ^{1}H-NMR (DMSO-d_6, 500 MHz): δ 3.28–3.34 (m, 2H, H-5`$_a$, H-5`$_b$), 3.68–3.75 (m, 2H, H-4`, H-3`), 4.02 (dist. t, 1H, $J_{OH5`,\ 5`a}$ 8.6 Hz, $J_{OH5`,\ 5`b}$ 6.1 Hz, OH-5`, exchangeable with $D_2O$), 4.37 (d, 1H, $J_{OH3`,H3`}$, 7.6 Hz, OH-3`), 4.18 (d, 1H, $J_{OH4`,H4`}$, 6.8 Hz, OH-4`), 4.48–4.59 (m, 3H, H-2`, $PhCH_2$), 4.94 (d, 1H, $J_{2`,\ OH2`}$ 7.1 Hz, OH-2`, exchangeable with $D_2O$), 5.63 (dist. t, 1H, $J_{1`,\ OH1`}$ 6.9 Hz, $J_{1`,\ 2`}$ 1.5 Hz, H-1`), 6.24 (d, 1H, $J_{1`,\ OH1`}$ 7.6 Hz, OH-1`, exchangeable with D_2O), 7.18 (dist. t, 1H, *J* 6.9 Hz, *J* 7.6 Hz, Ph-H) 7.27 (t, 2H, *J* 7.6 Hz, Ph-H), 7.42 (d, 2H, *J* 6.8 Hz, Ph-H), 8.27 (s, 1H, quin-H_6), 9.37 (s, 1H, quin-H_9). *Anal*. Calcd

for $C_{21}H_{20}Cl_2N_4O_5$, C, 52.62; H, 4.21; N, 11.69. Found: C, 52.14; H, 3.96; N, 11.68.

4-Benzyl-[1,2,4]triazolo[4,3-a]quinoxaline-1-carbaldehyde (10). A suspension of **7a** (2 g, 3.0 mmol) in water (100 mL) was treated with a solution of sodium metaperiodate (2.6 g, 12.5 mmol) in water (25 mL). The reaction mixture was stirred at room temperature for 4 h and then left overnight in the dark. The product (0.6, 70% was collected, washed with water, dried, and crystallized from ethanol to give **12** as colorless crystals mp 120–121°C, R_f 0.70 (4:1 ethylacetate: *n*-hexane); IR (KBr); ν 1680 (C=O), 2800–2900 (OC–H) cm^{-1}; ^{1}H-NMR ($CDCl_3$, 500 MHz): δ 4.78 (s, 2H, $PhCH_2$), 7.17 (t, 1H, *J* 6.8 Hz, Ph-H), 7.29 (t, 2H, *J* 7.6 Hz, Ph-H), 7.61 (d, 2H, *J* 7.6 Hz, Ph-H), 7.75 (m, 2H, quin-H_7, quin-H_8), 8.19 (d, 1H, $J_{6,7}$ 7.6 Hz, quin-H_6), 9.4 (d, 1H, $J_{9,8}$ 8.4 Hz, quin-H_9), 10. 47 (s, 1H, CHO). *Anal*. Calcd for $C_{17}H_{12}N_4O$: C, 70.82; H, 4.20; N, 19.43. Found: C, 70.52; H, 4.41; N, 19.23.

1-(D-Manno-pentitol-1-yl)-4-benzoyl[1,2,4]triazolo[4,3-a] quinoxaline (11). To a solution of 1-(2-benzylquinoxalin-3-yl) hydrazine **1** (2.50 mmol) in methanol (25 mL), D-mannose sugar (0.625 g, 2.50 mmol) and one drop of HCl (33%) were added. The reaction mixture was heated under reflux on boiling water bath for 1 h, left to cool at room temperature, and then a solution of bromine (0.13 mL, 2.50 mmol) in methanol (5.0 mL) was added drop wise with stirring for one day. A mixture of ethanol (3 mL) and pyridine (0.5 mL) was added, volatile components were evaporated in vacuum at 60°C. The residue was treated with ethanol (95%, 10 mL), then left to cool at room temperature. The crude product that precipitated out was collected by filtration, then washed by ethanol. The crude product was crystallized from ethanol to afford colorless crystals, (0.61 g; 59.5%); mp 227–228° C; ^{1}H-NMR (DMSO-d_6, 500 MHz): δ 3.52–3.85 (m, 5H, H-3`, H-4`, H-5_a`, H-$5`_b$, OH-5`, exchangeable with $D_2O$), 4.42–4.51(m, 4H, H-2`, OH-2`, OH-3`, OH-4`, exchangeable with $D_2O$), 5.51 (m, 1H, H-1`), 6.49 (d, 1H, $J_{OH\text{-}1`,1`}$ 6.1 Hz, OH-1`, exchangeable with D_2O), 7.55–7.58 (m, 2H, Ph-H), 7.73–7.76 (m, 2H, Ph-H), 7.86 (dis. t, 1H, *J* 7.4 Hz, *J* 6.8 Hz Ph-H), 8.0–8.02 (m, 2H, quin-H_7, quin-H_8), 8.13 (d, 1H, *J* 8.4 Hz, quin-H_6), 8.85 (d, 1H, *J* 8.4 Hz, quin-H_9). ^{13}C-NMR (DMSO-d_6, 125.7 MHz): δ 64.25, 66.55, 69.40, 69.83, 71.17, 119.91, 126.85, 128.58, 129.67, 130.86, 130.94, 131.50, 134.82, 135.70, 143.55, 149.71, 153. 16, 190.91(C=O). EI-MS: m/e 424.14 [M+]. *Anal*. Calcd for $C_{21}H_{20}N_4O_6$: C, 59.43; H, 4.75; N, 13.20. Found: C, 59.21; H, 4.71; N, 13.45.

D-Fructose (3-benzylquinoxalin-2-yl) hydrazones (12). To a solution of **1** (2.50 mmol) and fructose (2.50 mmol) in methanol (25 mL), one drop of HCl was added. The mixture was heated under reflux on water-bath for 1 h and left to cool. The pale red crystals that precipitated out was collected by filtration (0.94 g; 91.6%); mp 185–186°C. R_f 0.51 (7:3 ethylacetate to *n*-hexane). IR (KBr); ν 3297 (NH, OH) and 1660 cm^{-1} (C=N); ^{1}H-NMR (DMSO-d_6, 500 MHz): δ 3.45–3.69 (m, 5H, H-$1`_a$, H-$1`_b$, H-5`, H-$6`_a$, H-$6`_b$), 4.05 (s, 2H, $PhCH_2$), 4.31 (d, 1H, $J_{OH4`,4`}$ 7.6 Hz, OH-4`, exchangeable with D_2O), 4.36–4.42 (m, 2H, H-4`, OH-6` exchangeable with D_2O), 4.56 (d, 1H, $J_{OH5`,5`}$ 5.3 Hz, OH-5`, exchangeable with $D_2O$), 4.73 (d, 1H, $J_{OH3`,3`}$ 7.6 Hz, OH-3`, exchangeable with D_2O), 4.86 (d, 1H, *J* 7.6 Hz, H-3`), 5.11 (dist. t, 1H, *J* 6.1 Hz, *J* 4.6 Hz, OH-1`, exchangeable with D_2O), 7.07, 7.15 (2 t, 2H, Ph-H), 7.23 (t, 3H, *J* 7.6 Hz, Ph-H), 7.28–7.35 (m, 3H, quin-H_6, quin-H_7, quin-H_8), 7.50–7.54 (m, 1H, *J* 5.3 Hz, *J* 12.9 Hz, quino-H_9), 10.96 (s, 1H, N–H, exchangeable with D_2O); ^{13}C-NMR (DMSO-d_6, 125.7 MHz): major isomer δ 40.0 ($PhCH_2$), 58.58, 64.48, 69.08, 71.66, 71.88, 122.49, 126.73, 128.64, 128.70 129.75, 129.94, 132.36, 132.72, 138.24, 144.42, 159.75, aromatic carbons for the major isomer, 171.32 (C-2`); minor isomer δ 40.0 ($PhCH_2$), 63.07, 64.29, 70.56, 71.96, 73.21, 122.56, 126.58, 128.58, 128.46, 129.75, 130.01, 132.36, 132.72, 138.31, 144.42, 160.13, aromatic carbons for the minor isomer, 169.54 (C-2`). *Anal*. Calcd for $C_{21}H_{24}N_4O_5$: C, 61.15; H, 5.87; N, 13.58. Found: C, 60.88; H, 6.69; N, 13.72.

Method of calculations. A geometry optimization method for suitable conformers of the open and cyclic, syn-isomers and anti-isomers of **12** was performed on the solution phase using the DMSO as a solvent in the continuum solvation method [18,19] using the DFT/B3LYP/6-31++G** level incorporated in Gaussian 03 package [20]. This method and basis set were found to give accurate molecular geometries [21]. Isomer populations were calculated from the following equations using the calculated solution energy [12]:

$$n_i = \exp\left(-\frac{\Delta G_i}{RT}\right)$$

$$\Delta G_i = G_i - G_j$$

$$N = n_A + n_B + n_C$$

$$\%_i = \frac{n_i}{N} * 100$$

where n_i is the ratio number of isomers of type i and j, ΔG_i is the energy difference of isomers i and j; j is an isomer chosen arbitrary; R is the gas constant (1.987 cal mol^{-1} K^{-1}), and T is the absolute temperature (289.15 K).

Biology. Agar-diffusion method was used for the determination of antibacterial and antifungal activity. From each of the test compounds in DMF (1 mg/mL), 75 µL was placed in a 6-mm-diameter well in gar plate seeded with the appropriate test organism in triplicates. Ampicillin trihydrate (10.0 µg/disc), Ciprofloxacin (5.0 µg/disc), Impenam (10.0 µg/disc) and Clotrimazole (100.0 µg/disc) were used as standard antibacterial and antifungal agents, respectively. DMF alone showed no IZ. The plates were incubated at 37°C for 24 h. The results were recorded for each tested compound and the reference drugs as the average diameter of IZ of bacterial growth in mm (Table 1).

Molecular docking. Molecular docking studies were carried out to understand the molecular binding modes of the active synthesized compounds toward three different biological targets belonging to focused microorganisms. Target compounds were docked against three biological targets including the crystal structures of enoyl-acyl carrier protein reductase (FabI) (Protein Data Bank (PDB) code 1C14) as *E. coli* promising target, dihydropteroate synthetase (PDB code 1 AD4) as *S. aureus* promising target, and *N*-myristoyl transferase (PDB code 1IYL) as *C. albicans* promising target [22]. The proteins were considered without co-crystallized ligands for the purpose of the docking simulations. Before screening the active compounds, the docking protocol was validated by running the simulation only using the bound ligands and low rmsd between docked and crystal conformations. AutoDock 3.0 [23] and MOE [24] softwares were used for all docking calculations. The AutoDockTools package [24] was employed to generate the docking input files

and to analyze the docking results. A grid box size of $90 \times 90 \times 90$ points with a spacing of 0.375 Å between the grid points was generated that covered almost the entire protein surface. Ligands were fully flexibly docked. All non-polar hydrogens and crystallographic water molecules were removed prior to the calculations. The docking grid was centered on the mass center of the bound trichostatin A (TSA). In each case, 100 docked structures were generated using genetic algorithm searches. A default protocol was applied with an initial population of 50 randomly placed conformations, a maximum number of 2.5×105 energy evaluations, and a maximum number of 2.7×104 generations. A mutation rate of 0.02 and a crossover rate of 0.8 were used. Heavy atom comparison rmsd values were calculated, and initial ligand binding modes were plotted. Protein-ligand interaction plots were generated using MOE 2008.10.

Acknowledgment. HA gratefully acknowledge the support from the Deanship of Scientific Research at Taibah University, Al-Madinah Al-Munawarah, Saudi Arabia. The authors would like to thank chemical computing group for use of the MOE software.

REFERENCES AND NOTES

[1] Socha, A. M.; LaPlante, K. L.; Russell, D. J.; Rowley, D. C. Bioorg Med Chem Lett 2009, 19, 1504.

[2] Henen, M. A.; El Bialy, S. A. A.; Goda, F. E.; Nasr, M. N. A.; Eisa, H. M. Med Chem Res 2012, 21, 2368.

[3] Suresh, M.; Lavanya, P.; Suchakar, D.; Vashu, K.; Rao, C. V. J Chem Pharm Res 2010, 2, 497.

[4] Badran, M. M.; Abouzid, K. A. M.; Hussein, M. H. M. Arch Pharm Res 2003, 26, 107.

[5] Carta, A.; Piras, S.; Loriga, G.; Paglietti, G. Mini-Rev Med Chem 2006, 6, 1179.

[6] Ingle, R. G.; Marathe, R. P. Pharmacophore 2012, 3, 109.

[7] Ajani, O. O.; Obafemi, C. A.; Nwinyi, O. C.; Akinpelu, D. A. Bioorg Med Chem 2010, 18, 214.

[8] El-Sabbagh, O. I.; El-Sadek, M. E.; Lashine, S. M.; Yassin, S. H.; El-Nabtity, S. M. Med Chem Res 2009, 18, 782.

[9] Abbas, H. A. S.; Hafez, H. N.; El-Gazzar, A. R. B. A. Eur J Med Chem 2011, 46, 21.

[10] Srivastava, R.; Bhargava, A.; Singh, R. K. Bioorg Med Chem Lett 2007, 14, 6239.

[11] Sarabia, F.; Martín-Ortiz, L. Tetrahedron 2005, 61, 11850.

[12] Amer, A.; Salah, M.; Khattab, S. N.; Yassen, S.; Langer, V.; El Massry, A. M. Carbohydr Res 2010, 345, 2474.

[13] Khattab, S. N.; Yassin, S.; Bekhit, A.; ElMassry, A. M.; Langer, V.; Amer, A. Eur J Med Chem 2010, 45, 4479.

[14] Khattab, S. N.; Yaseen, S.; El Faham, A.; ElMassry, A. M.; Amer, A. J Heterocycl Chem 2007, 44, 617.

[15] Yaseen, S.; Kattab, S. N.; Bekhit, A.; Amer, A. Bioorg Med Chem Lett 2006, 16, 1753.

[16] He, C.; Zhang, X.; Huang, R.; Pan, J.; Li, J.; Ling, X.; Xiong, Y.; Zhu, X. Tetrahedron Lett 2014, 55, 4458.

[17] Schleinitz, K. D.; Westphal, G.; Surkau, A.; Lochner, D. J Prakt Chem 1980, 322, S199.

[18] Barone, V.; Cossi, M. J Phys Chem A 1998, 102, 1995.

[19] Cossi, M.; Rega, N.; Scalmani, G.; Barone, V. J Comput Chem 2003, 24, 669.

[20] Gaussian 03, Revision B.01, Gaussian, Inc.: Pittsburgh, PA, 2003.

[21] Hasanein, A.; Senior, S. A. Bull Chem Soc Jpn 2007, 80, 307.

[22] Berman, H. M.; Westbrook, J.; Feng, Z.; Gilliland, G.; Bhat, T. N.; Weissig, H.; Shindyalov, I. N.; Bourne, P. E. Nucleic Acids Res 2000, 28, 235.

[23] Morris, G. M.; Goodsell, D. S.; Halliday, R. S.; Huey, R.; Hart, W. E.; Belew, R. K.; Olson, A. J. J Comput Chem 1998, 19, 1639.

[24] Molecular Operating Environment (MOE), Chemical Computing Group Inc., 2012. www.chemcomp.com. Accessed March 2013.